Journal of Inflammation Research

Dovepress
open access to scientific and medical research

Open Access Full Text Article

ORIGINAL RESEARCH

Unveiling Immune Infiltration Characterizing Genes in Hypertrophic Cardiomyopathy Through Transcriptomics and Bioinformatics

Jianmin Gong[1,2,*], Bo Shi[1,3,*], Ping Yang[1], Adeel Khan[4], Tao Xiong[2], Zhiyang Li[1]

[1]Department of Clinical Laboratory, Nanjing Drum Tower Hospital, Nanjing Drum Tower Hospital Clinical College of Nanjing Medical University, Nanjing, 210000, People's Republic of China; [2]College of Life Science, Yangtze University, Jingzhou, 434025, People's Republic of China; [3]Department of Clinical Laboratory, Nanjing Jiangning Hospital of Chinese Medicine (CM), Nanjing, 211100, People's Republic of China; [4]Department of Biotechnology, University of Science and Technology Bannu, Bannu, 28100, Islamic Republic of Pakistan

*These authors contributed equally to this work

Correspondence: Tao Xiong, College of Life Science, Yangtze University, Jingzhou, 434025, People's Republic of China, Tel +8613872387410, Email xiongtao@yangtzeu.edu.cn; Zhiyang Li, Department of Clinical Laboratory, Nanjing Drum Tower Hospital, Nanjing Drum Tower Hospital Clinical College of Nanjing Medical University, Nanjing, 210008, People's Republic of China, Tel +8618951703765, Email lizhiyang@nju.edu.cn

Background: Hypertrophic cardiomyopathy (HCM) is a dominantly inherited disease associated with sudden immune cell associations that remain unclear. The aim of this study was to comprehensively screen candidate markers associated with HCM and immune cells and explore potential pathogenic pathways.

Methods: First, download the GSE32453 dataset to identify differentially expressed genes (DEGs) and perform Gene Ontology and pathway enrichment analysis using DAVID and GSEA. Next, construct protein-protein interaction (PPI) networks using String and Cytoscape to identify hub genes. Afterward, use CIBERSORT to determine the proportion of immune cells attributed to key genes in HCM and conduct ROC analysis based on the external dataset GSE36961 to evaluate their diagnostic value. Finally, validate the expression of key genes in the hypertrophic cardiomyocyte model through qRT-PCR using data from the HPA database.

Results: Comprehensive analysis revealed that there were 254 upregulated genes and 181 downregulated genes in HCM. The enrichment study underscored pathways of inflammatory signaling, including MAPK and PI3K-Akt pathways. Pathways abundant in genes associated with HCM encompassed myocardial contraction and NADH dehydrogenase activity. Additionally, the analysis of immune infiltration revealed a notable increase in macrophages, NK cells, and monocytes in the HCM group, showing statistically significant variances in CD4 memory resting T cell infiltration when compared to the healthy control group. Within the validation dataset GSE36961, the Area Under the Curve (AUC) scores for eight crucial genes (FOS, CD86, CD68, BDNF, PIK3R1, PLEK, RAC2, CCL2) each exceeded 0.8. The HPA database revealed the positioning traits and paths of these eight crucial genes in smooth muscle cells, myocardial cells, and fibroblasts. The outcomes of the qRT-PCR were aligned with the sequencing findings.

Conclusion: Bioinformatics analysis unveiled pivotal genes, pathways, and immune involvement, illuminating the molecular underpinnings of HCM. These findings suggest promising therapeutic targets for clinical applications.

Keywords: hypertrophic cardiomyopathy, bioinformatic, immune cells infiltration, biomarker

Introduction

Hypertrophic cardiomyopathy (HCM) is a heterogenic genetic disease most commonly caused by sarcomeric mutations that lead to left ventricular hypertrophy, fibrosis, hypercontractility and reduced compliance.[1] The intricate nature of hypertrophic cardiomyopathy involves a combination of diastolic dysfunction, myocardial ischaemia, and outflow tract obstruction and arrhythmias caused by the displacement of the mitral valve in the front. From a clinical standpoint, the symptomatology exhibits a wide range, encompassing no discernible symptoms as well as palpitations, dyspnoea, diminished exercise capacity, chest discomfort, syncope, and even abrupt demise.[2] Epidemiological studies indicate that at least 1 in every 500 individuals is affected by hypertrophic cardiomyopathy, while 1 in every 200 individuals is

Received: 11 December 2023
Accepted: 1 May 2024
Published: 17 May 2024

either affected by it or has a genetic predisposition.[3] Despite functional and genome-wide association studies (GWAS) suggesting an association between the FHOD3 gene and myocardial hypertrophy, no pathogenic variants directly related to hypertrophic cardiomyopathy have been identified.[4] While significant progress has been made in the diagnosis through the use of echocardiography, clinical diagnosis still faces several challenges, including the diversity of clinical manifestations, uncertainty in imaging examinations, consideration of genetic factors, and overlap with other cardiac diseases.[5–7]

The immune system plays a crucial role in maintaining optimal cardiac function, with particular significance in HCM. It triggers an unconventional inflammatory response and subsequent myocardial restructuring following injury.[8,9] Studies have demonstrated that individuals afflicted with HCM exhibit inflammatory cell infiltration and fibrosis within their myocardium.[10] Previous investigations have predominantly linked HCM with myonodal gene variants, notably MYH7 and MYBPC3.[11] Nevertheless, numerous unidentified potential mutations endure, while the intricate signaling pathways and regulatory networks responsible for HCM's pathogenesis remain inadequately understood. Hence, there is an imperative need to explore and elucidate potential genes and biological pathways relevant to HCM pathogenesis, essential for accurate disease diagnosis, treatment, and prevention.

Bioinformatics analysis, leveraging microarray and high-throughput sequencing technologies, facilitates the identification of new genes and biomarkers for various diseases. The Gene Expression Omnibus (GEO) database harbors a wealth of published data, offering opportunities for deeper exploration of molecular processes. In our study, we conducted an extensive analysis of differential genes between HCM patients and healthy controls using GEO datasets, systematically identifying key genes associated with HCM and their biological functions. Additionally, we employed the CIBERSORT algorithm to assess immune cell subpopulations and analyze immune infiltration in HCM tissues compared to normal tissues (Figure 1). Our research introduces novel concepts and perspectives to discover new HCM biomarkers and investigate potential causative factors.

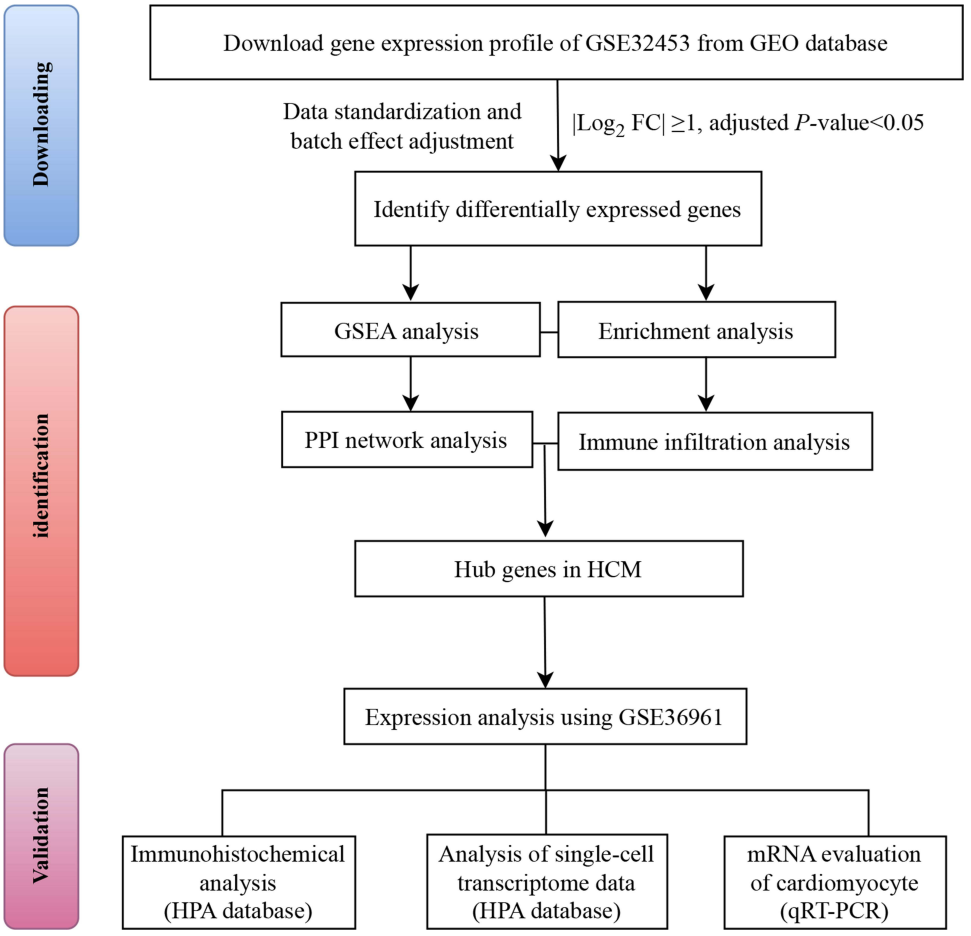

Figure 1 Workflow chart of this study.

Materials and Methods

Data Collection and Processing

Our search, conducted at the National Center for Biotechnology Information, relied on the accessible GEO database (https://www.ncbi.nlm.nih.gov/geo/). We specifically targeted publicly available studies meeting stringent criteria: (1) gene expression data sets encompassing both HCM and normal heart tissue samples, (2) data exclusively from Homo sapiens, and (3) consistent sample information devoid of missing values. Our selection for analysis comprised GSE32453 and GSE36961. GSE32453, generated on the GPL6104 platform using the Illumina humanRef-8 v2.0 expression beadchip, encompassed cardiac myectomies/biopsies from 8 HCM patients and 5 without HCM. In addition, GSE36961 included 109 HCM patients and 36 non-HCM patients, using the GPL15389 platform (Illumina HumanHT-12 V3.0 expression beadchip) as a validation set to evaluate hub gene expression levels.

Integrated Analysis of DEGs

After preprocessing the microarray data from GSE32453 and GSE36961 through GEO2R (https://www.ncbi.nlm.nih.gov/geo/geo2r/), an alignment in the medians of the 13 sample and 145 sample datasets was observed. This congruence indicates the high quality and robust experimental consistency of the microarray data (Supplementary Figure 1A and 1B). Subsequently, differentially expressed genes (DEGs) between the normal control group and hypertrophic cardiomyopathy patients were chosen for further analysis. Data processing, executed using R software (Version 4.2.3), involved downloading primary GEO matrix files and normalizing them with the "limma" R package. Upregulated DEGs were identified by log2FC > 1, while downregulated DEGs were determined by log2FC < −1. Differential expression visualization utilized both a volcano plot and heatmap.

Bio-function Enrichment and Gene Set Enrichment Analysis

The Database for Annotation, Visualization, and Integrated Discovery (DAVID) stands as an online analytical tool that facilitates the practical analysis of genes obtained from genomic research. Utilizing the resources provided by DAVID, we conducted an analysis involving Gene Ontology (GO) functions and Kyoto Encyclopedia of Genes and Genomes (KEGG) pathway enrichment. Our investigation specifically focused on Gene Ontology terms associated with biological processes (BP), molecular functions (MF), and cellular components (CC). Notably, we observed a statistically significant enrichment level in the biological functions linked to GO terms and KEGG pathways. The cluster Profiler package, accessible on the Molecular Characterization Database website (https://www.gsea-msigdb.org/gsea/msigdb/index.jsp), was utilized to carry out Gene Set Enrichment Analysis (GSEA) and acquire the relevant analysis.

Immune Infiltration Analysis Between HCM Patients and Healthy Controls

The CIBERSORT web tool (http://CIBERSORT.stanford.edu/) was utilized to assess immune cell infiltration and investigate the immune microenvironment in the disease, utilizing normalized gene expression data from both disease and control samples. The reference set comprised 22 genes associated with immune cells (LM22) and underwent 1000 permutations. The outcomes of immune cell infiltration were depicted through clustered heatmaps and stacked plots. Spearman's rank sum analysis was utilized to calculate correlations among individual immune cells. GraphPad software (version 9.5.1) was employed to visualize the relationships between immune cell infiltration and the percentage of immune cells in patients with HCM and healthy controls.

Construction of Protein–Protein Interaction Network

The STRING database (https://string-db.org/) was used to gain insight into the protein–protein interaction (PPI) network by inputting the significant common Differentially Expressed Genes (DEGs). After eliminating the disconnected nodes, the PPI network was built using Cytoscape version 3.9.1 software (https://cytoscape.org/). The cytoHubba plug-in was employed to pinpoint crucial modules linked to HCM, establishing the Molecular Complex Detection (MCODE) score threshold as > 5.0.Intramodular connectivity (IC) denotes the strength of connections among genes within the module,

where higher IC indicates greater significance of genes within the module. Consequently, genes exhibiting high IC were identified as hub genes. Visualization was conducted using Cytoscape.

Confirmation and Identification of Predictive Genes

We verified the expression profiles of hub genes using the integrated validation dataset of GSE36961. The R packages "limma" and "ggpubr" (https://cran.r-project.org/web/packages/ggpubr/) were utilized to evaluate the variations in expression between the HCM and control groups. The "pROC" package was utilized for conducting ROC curve analysis. Subsequently, immunohistochemical and single-cell transcriptome information was obtained from the Human Protein Atlas (HPA) database (https://www.proteinatlas.org/) to determine the positioning characteristics of essential genes in human heart muscle. The exact information was obtained from the HPA database. (Supplementary Table 1 and 2).

Establishment of Cardiac Mast Cell Model

The H9c2 rat cardiomyocyte cell line was procured from the American Type Culture Collection (ATCC; Manassas, VA, USA) and cultured in high-glucose Dulbecco's Modified Eagle's Medium (DMEM) supplemented with 10% fetal bovine serum (FBS) and 1% penicillin/streptomycin (P/S). The cells were maintained under 5% CO_2 at 37°C, and the culture medium was refreshed every 2 days. Next, the H9c2 cells were seeded onto cell slide-covered 24-well plates and subjected to a 24 h treatment with 1 μmol/L of angiotensin II (Ang II) (Aladdin, Shanghai, China) upon reaching 70% cell density. Subsequently, the cells underwent a 15 min treatment with 4% paraformaldehyde, followed by three successive five-minute rinses with 1× PBS buffer. This was succeeded by a 20 min treatment involving 1% Triton X-100 and 1% BSA in PBS buffer, followed by 35 min washes with 1×PBS buffer each. The cytoskeleton and nucleus were stained using TRITC Phalloidin and DAPI Staining Solution, respectively. Finally, the cell slides were sealed with mounting medium and examined under a fluorescence microscope. Furthermore, ImageJ (Version 1.54f) software was used to quantify the relative surface area of cardiomyocytes. Additionally, qRT-PCR was conducted to identify hallmark genes associated with cardiac hypertrophy: ANP, BNP, and β-MHC.

Quantitative Real-time Polymerase Chain Reaction (qRT-PCR) Analysis

We analyzed the mRNA levels of genes derived from the sequencing results in both HCM modelling and control cells. In accordance with the given instructions, the RNA-Quick Purification Kit (RN001, Yishan, Shanghai, China) was employed to extract total RNA from cells, which was then synthesized into cDNA using a HiScript IlI All-in-one RT SuperMix Perfect for qPCR (R333, Vazyme, Nanjing, China). The ChamQ Universal SYBR PCR Master Mix (Q711, Vazyme, Nanjing, China) was utilized for the precise identification of mRNAs. The GAPDH gene was employed as the internal benchmark. Supplementary Table 3 provided comprehensive details on primer sequences.

Statistical Analysis

Quantitative variables were expressed as mean ± standard deviation (SD). Statistical significance was assessed using the Student's *t*-test in SPSS version 26.0 (IBM Corp., Armonk, New York, USA). Moreover, the Wilcoxon test and Kruskal-Walli's test were employed for pairwise and multiple group comparisons, respectively. Correlation coefficients were calculated using Spearman's analysis, with a p-value of less than 0.05 indicating statistical significance.

Results

Identification of DEGs

The GSE32453 dataset revealed a substantial disparity in the expression of 435 genes between normal and HCM. Out of these, 254 genes showed an increase in expression, while 181 genes showed a decrease in expression in HCM. Figure 2A and B display the volcano map and heatmap.

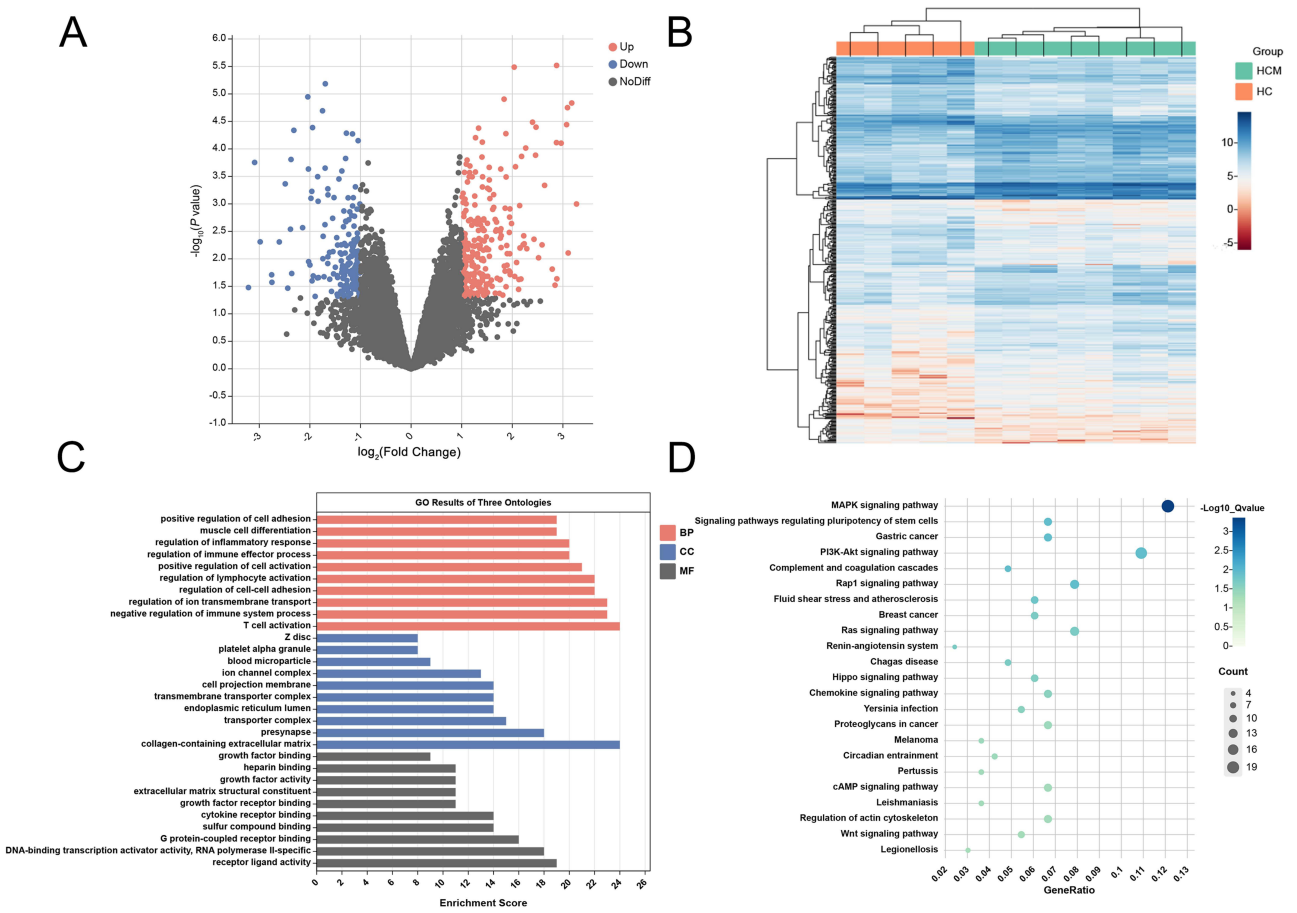

Figure 2 Screening and biological function analysis of differentially expressed genes between HCM and healthy controls. (**A**) Volcano plots of differentially expressed genes between control and HCM groups, red nodes indicate upregulation, blue nodes indicate downregulation and gray nodes indicate no significant differences. (**B**) The heatmap of differentially expressed genes between the control and HCM groups. (**C**) Analysis of differential gene GO enrichment in HCM. (**D**) Enrichment analysis of the differential gene KEGG signaling pathway in HCM.

Exploration of GO Term and KEGG Pathway Enrichment in DEGs

GO analyses elucidated the biological functions of GEGs shared by hypertrophic cardiomyopathy. A total of 285 GO terms were associated with these common DEGs (Supplementary Table 4). These included T cell activation in biological processes, negative regulation of immune system processes, and cellular components involving the collagen-containing extracellular matrix and presynaptic. Notably, molecular functions included receptor ligand activity, DNA-binding transcriptional activator activity, and RNA polymerase II-specific functions (Figure 2C). Further pathway network analysis was performed on the important pathways identified in the KEGG pathway enrichment analysis (Supplementary Table 5). These DEGs were mainly associated with immune cell-related signalling pathways, such as the MAPK signalling pathway, the signalling pathway regulating stem cell pluripotency, and the PI3K-Akt signalling pathway. Overall, most of the functions attributed to differentially expressed genes were enriched for myoblast differentiation and immune cells (Figure 2D).

Signaling Pathways Identified by GSEA

GSEA was conducted using data from HCM patients and controls in the GSE32453 database. GESA-KEGG results revealed that HCM group genes were mainly enriched in the cardiac muscle contraction signaling pathway, propanoate metabolism signaling pathway, citrate cycle TCA cycle signaling pathway, oxidative phosphorylation signaling pathway and proteasome signaling pathway (Figure 3A). Of these, the myocardial contraction signaling pathway and the oxidative phosphorylation signaling pathway had the higher normalized enrichment score (NES) (NES=3.691, *P*=0.012; NES=3.811, *P*=0.012) (Figure 3B). GESA-GO analysis showed significant enrichment of

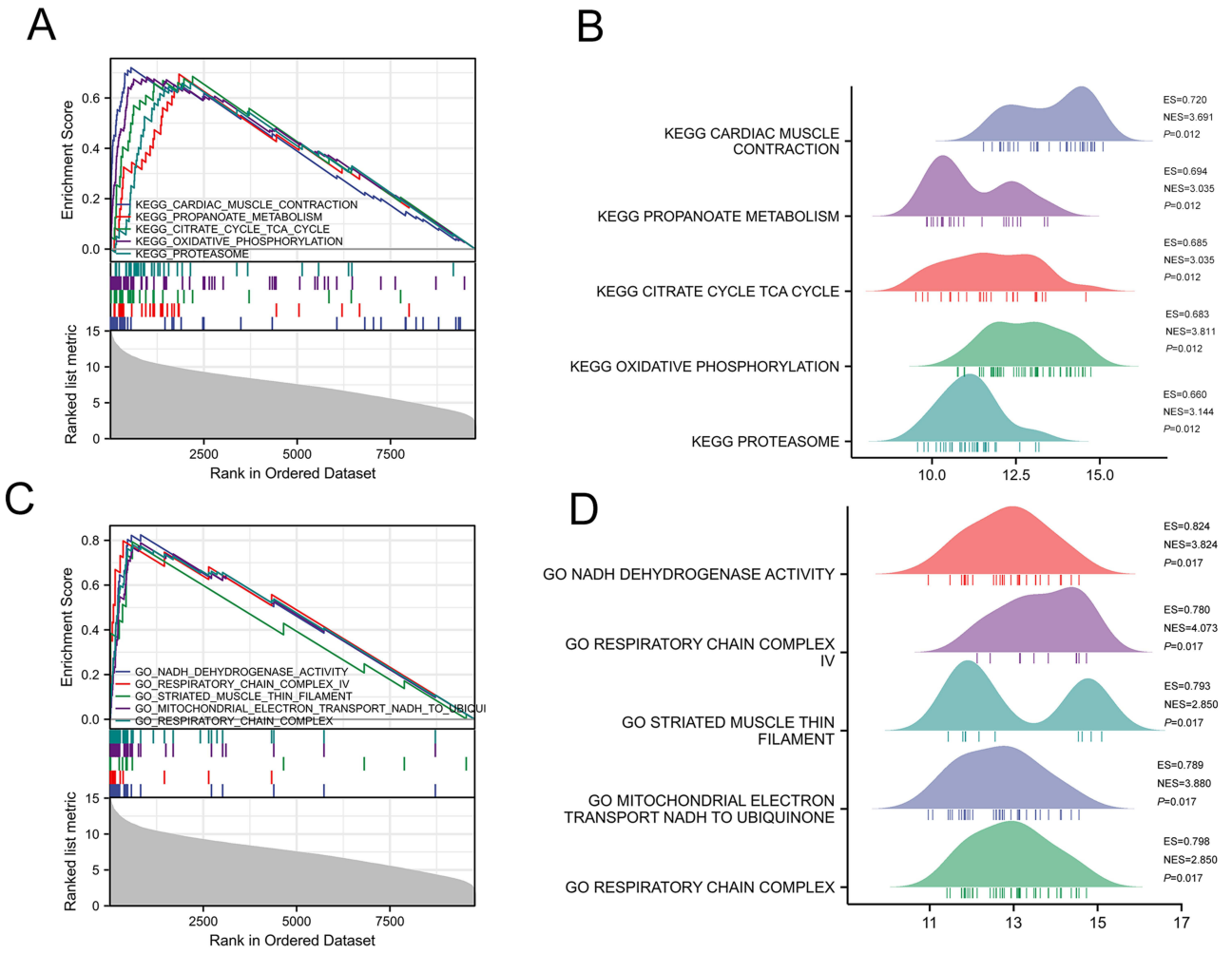

Figure 3 Results of GESA in HCM of GSE32453 database. (**A**) KEGG enrichment analyses using GSEA. (**B**) Results for GESA-KEGG ridgeline plots. (**C**) GO enrichment analyses using GESA. (**D**) Results for GESA-GO ridgeline plots.

HCM genes in the NADH dehydrogenase activity, respiratory chain complex IV, striated muscle thin filament, mitochondrial electron transport NADH to ubiquinone and respiratory chain complex (Figure 3C). Among them, respiratory chain complex IV had the highest normalized enrichment score (NES=4.073, *P*=0.017) (Figure 3D).

Immune Infiltration Analyses

In each sample of the GSE32453 dataset, immune cells were mainly clustered in Macrophages, NK cells and monocytes (Figure 4A). Macrophages M0 and NK cells resting were more widely distributed and accounted for the majority of the samples (Figure 4B). The corheatmap result showed that mast cells resting and T cells gamma delta had a positive correlation. NK cells resting and T cells gamma delta, mast cells resting and macrophages M0, and dendritic cells activated and macrophages M1 had a significant negative correlation (Figure 4C). Compared with normal tissue, immunocyte histograms show a statistically significant difference in T cells CD4 memory resting infiltration in myocardial tissue of HCM patients and healthy controls. In myocardial tissues of HCM patients, there was an increase in T cells CD4 memory activated, T cells gamma delta, NK cells resting, monocytes and macrophages M0, while T cells CD4 memory resting and macrophages M2 were decreased (Figure 4D).

Analyzing DEGs in HCM Using a PPI Network

The DEG expression products in HCM were constructed by way of the STRING database to construct PPI networks. The PPI network composed of differential genes included 416 nodes and 890 edges (Figure 5A). Cytoscape software was used to

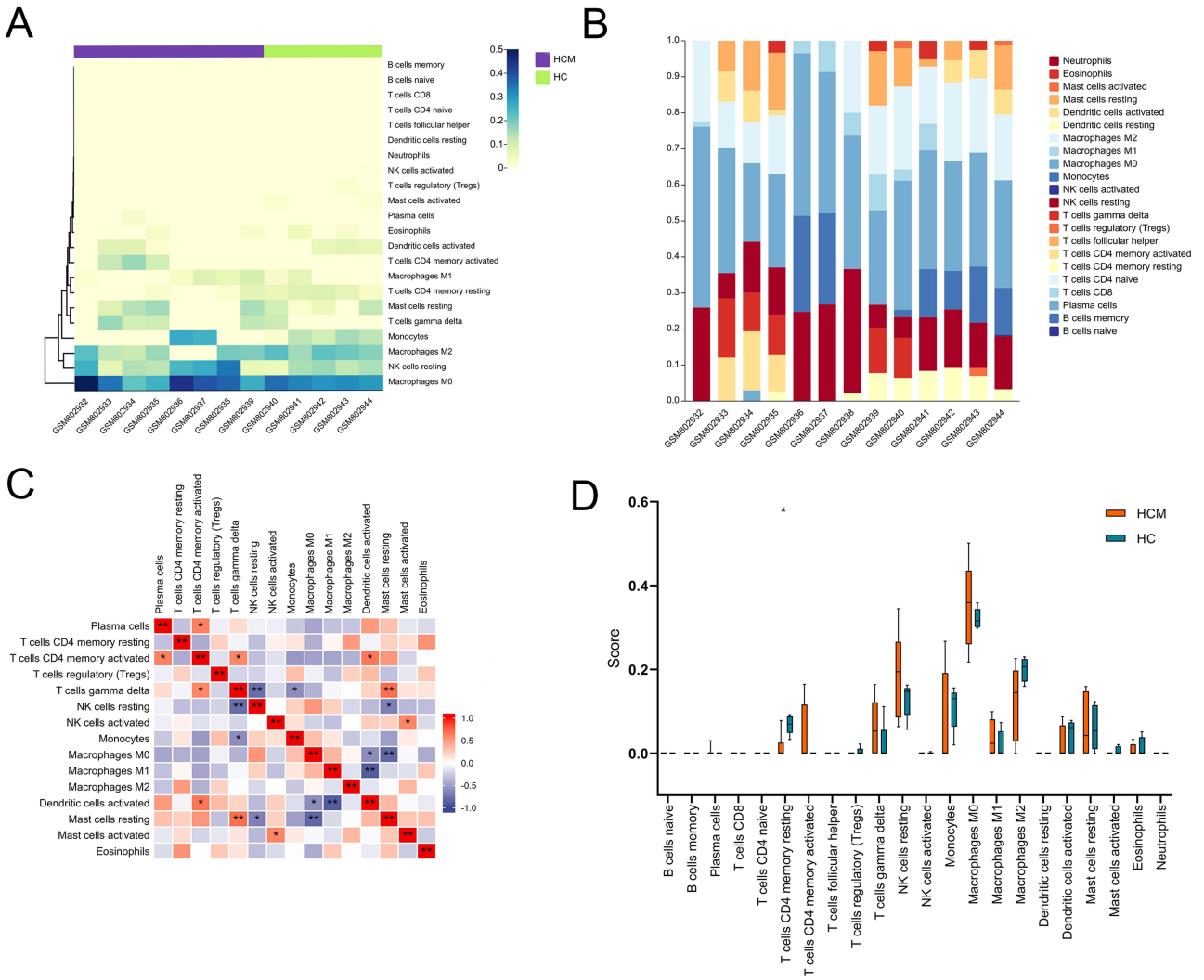

Figure 4 Immune infiltration analysis between HCM patients and healthy controls. (**A**) Clustering of twenty-two immune cells in HCM and healthy control samples. (**B**) The percentage of twenty-two subpopulations of immune cells for each sample in HCM and healthy controls. (**C**) Correlation analysis between twenty-two immune cells in HCM. (**D**) The difference of immune cells between HCM patients and healthy controls.

analyze the PPI network of differential genes, and the MCC algorithm with CytoHubba plug-in was used to filter out the top 10 genes in the degree ranking and define them as hub genes. Finally, we screened ten hub genes (IL2, FOS, CD86, CD68, CCL2, BDNF, RAC2, PLEK, PIK3R1, LCP2) (Figure 5B). The downregulated genes accounted for more of the hub genes (Table 1).

Validation and ROC Curve of Hub Genes

To assess the reliability of these hub gene expressions, GSE36961 dataset was used for validation of the expression level of the potential hub genes. The results showed that nine hub genes were significantly different between HCM and healthy controls. Among them, genes BDNF and PIK3P1 were significantly up-regulated in HCM myocardial tissues, and the expression of FOS, CD86, CD68, PLEK, RAC2, CCL2, and LCP2 was down-regulated in HCM myocardial tissues (Figure 6A). In parallel, we analyzed the results of ROC curves for these genes, in which genes with AUC>0.8 were identified as key genes. Finally, FOS, CD86, CD68, BDNF, PIK3P1, PLEK, RAC2 and CCL2 were defined as key genes associated with HCM (Figure 6B).

In addition to ROC analysis, expression of these eight key genes was evaluated using a combination of dataset, immunohistochemistry data and single-cell transcriptome data from the HPA database. We found that FOS and PIK3R1 genes occupied a high positive area but a low area of RAC2 in cardiac tissue. While CD86, CD68, BNDF, PLEK and

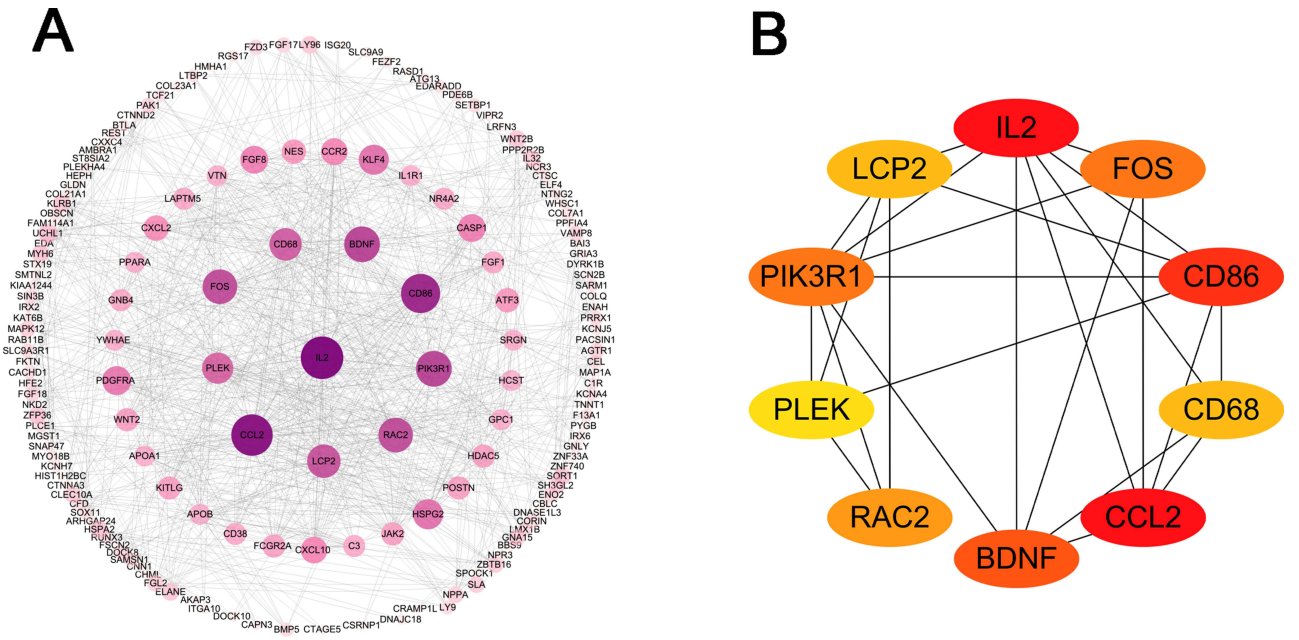

Figure 5 PPI network of DEGs extracted by MCODE. (**A**) The interaction network between proteins coded by DEGs was comprised of 416 nodes and 890 edges. The larger and darker the circle, the more important the gene. (**B**) Interaction of top 10 genes calculated by MCODE.

CCL2 expression were not detected in heart tissues. Subsequently, we analyzed the single-cell expression pattern and the developmental trajectory from the HPA database.

In Figure 7, FOS shows low expression in endothelial and fibroblast clusters, but increases notably in cardiomyocyte and smooth muscle cell clusters. CD68 has minimal expression across all clusters and is notably absent in most. Smooth muscle cells exhibit gradual elevation in CD86, PLEK, and RAC2 levels, while cardiomyocytes and endothelial cells show a partial decline in RAC2 concentrations. BNDF has high expression in cardiomyocyte clusters but trends lower in fibroblast clusters. PIK3R1 is notably high in all clusters except for endothelial and smooth muscle cells. CCL2 maintains consistently high expression in smooth muscle cells, endothelial cells, and fibroblasts, but decreases in cardiomyocytes, indicating distinct regulatory patterns across cell types. These findings highlight the dynamic expression patterns of crucial genes in cellular differentiation and function.

Expression Validation Through qRT-PCR

To validate our findings, we developed a cardiac mast cell model to investigate the expression of eight key genes. Using qRT-PCR, we demonstrated a significant upregulation of cardiac hypertrophy-associated genes—specifically ANP, BNP,

Table 1 Core Target Gene Information

Gene	Log_2FC	*P* value	Type
LCP2	−1.156	0.001	Down
FOS	−2.982	0.005	Down
BDNF	1.416	0.010	Up
RAC2	−1.243	0.012	Down
CD86	−1.459	0.020	Down
IL2	2.880	0.023	Up
PLEK	−1.268	0.025	Down
PIK3R1	1.083	0.034	Up
CD68	−1.240	0.041	Down
CCL2	−1.360	0.042	Down

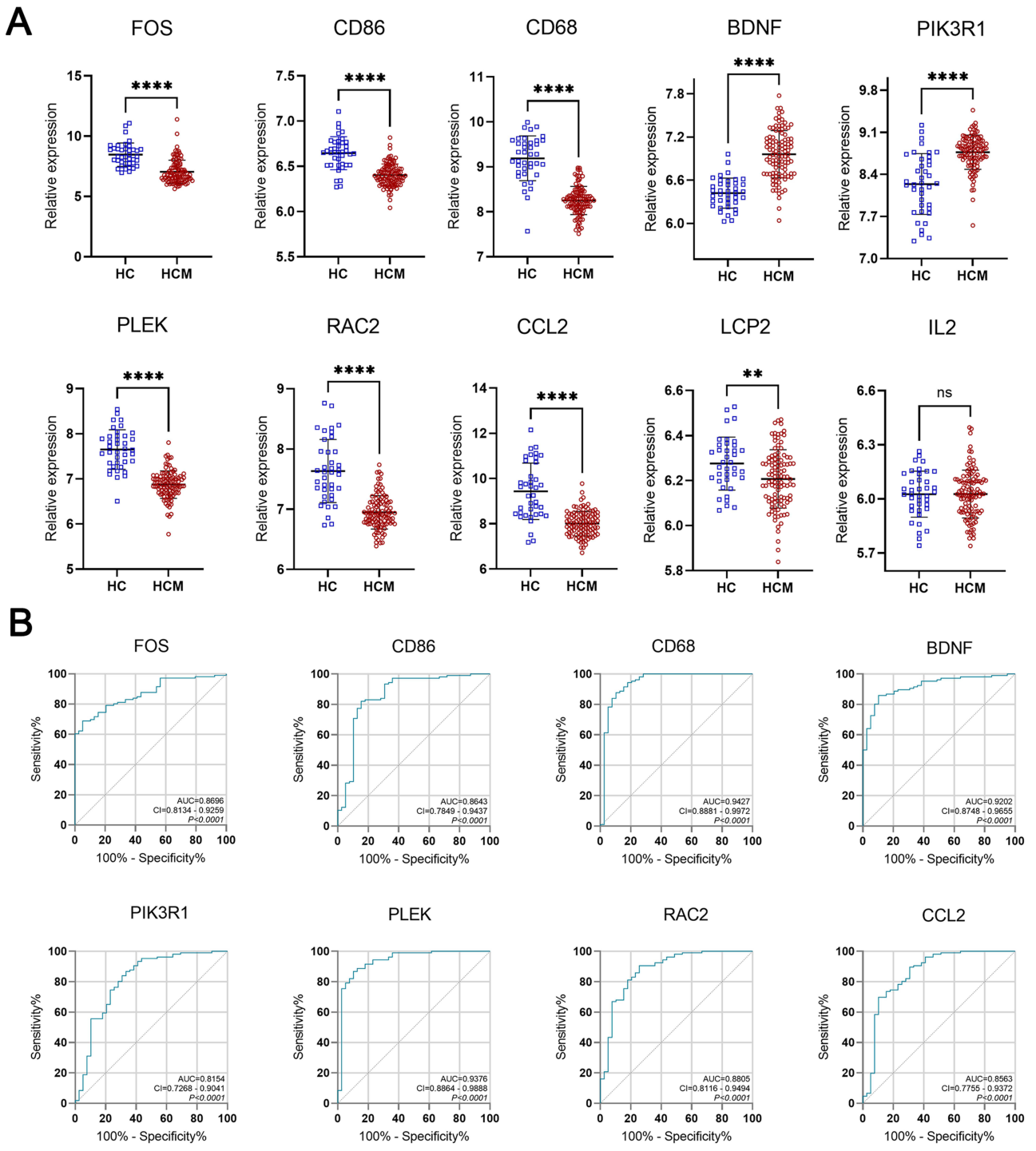

Figure 6 Predictive value of hub genes for HCM. (**A**) Hub genes expression in the GSE36961 dataset between the HCM and control group. (**B**) The ROC curves were shown in the validation set for eight key genes with AUCs > 0.8 in the GSE36961 dataset. Error bars indicate mean ± standard deviation. ***P*<0.01; *****P*<0.0001.

and β-MHC—in Ang II-exposed H9c2 cells (Supplementary Figure 2A–C). Furthermore, a notable increase in cell surface area was observed in the cardiac hypertrophy group compared to the control cells (Supplementary Figure 2D–F), confirming the successful establishment of a hypertrophic cardiomyocyte model.

Our qRT-PCR results indicated a significant upregulation of BDNF and PIK3P1, along with downregulation of CD86, PLEK, and RAC2 expression in the cardiac hypertrophy cell group, consistent with altered gene transcription. However, there were no discernible differences in FOS, CD68, and CCL2 expression between the groups. (Figure 8).

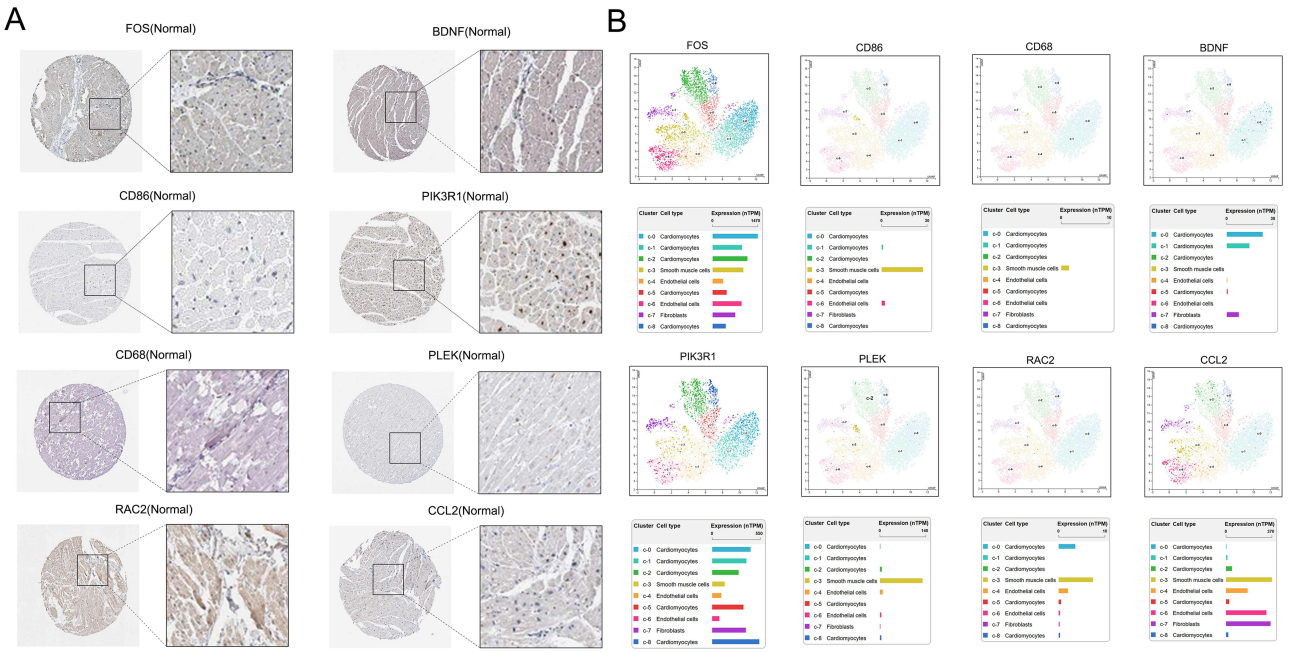

Figure 7 Subcellular localization of eight key genes. (**A**) The expression of the eight major genes for humans with normal cardiac tissue in the HPA database is determined by immunohistochemistry. (**B**) Transcriptome study of Single-cell for the eight major genes found in the HPA database.

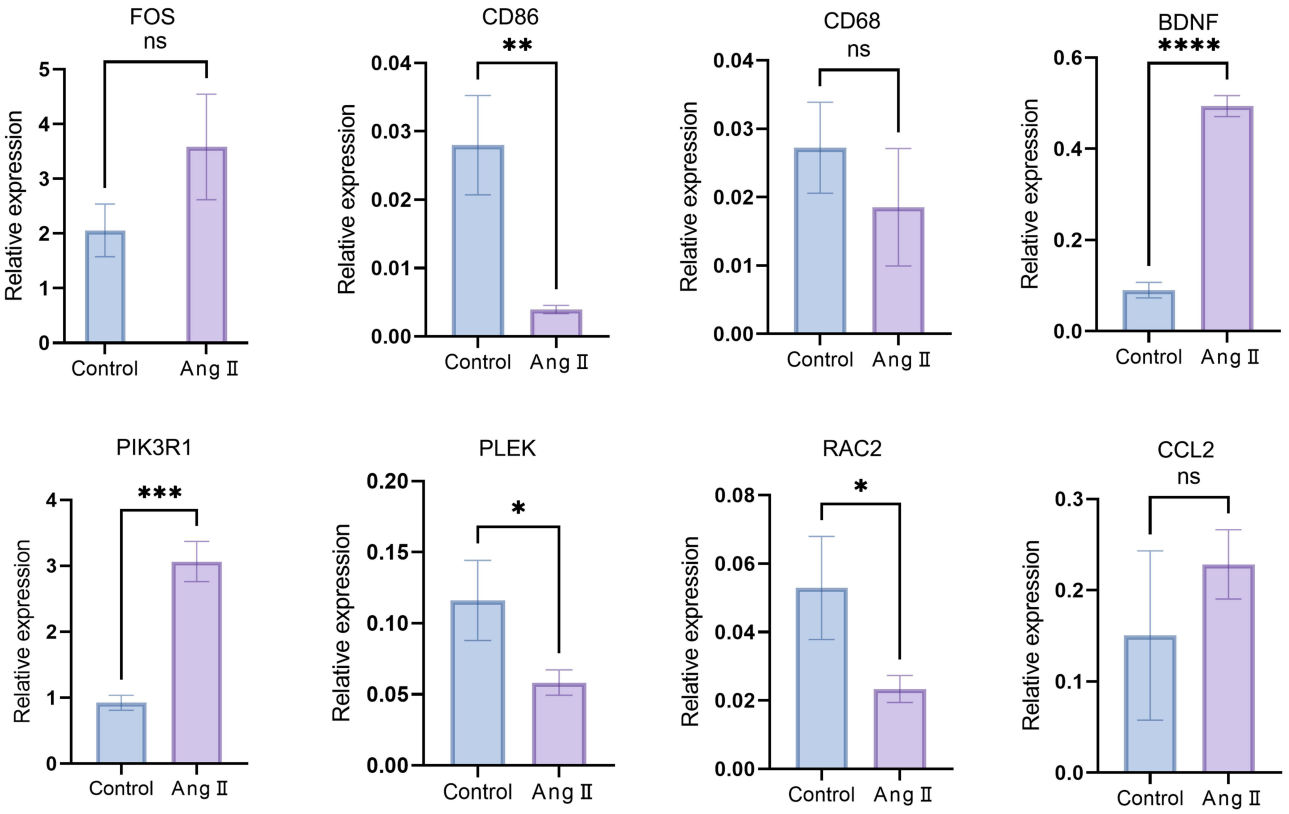

Figure 8 The mRNA levels of eight key genes in the H9c2 cells from cardiomegaly group and control group. Error bars indicate mean ± standard deviation. *P<0.05, **P<0.01; ***P<0.001, ****P<0.0001.

Discussion

This study screened 435 differentially expressed genes between HCM and healthy control myocardial tissues by analyzing the gene expression profiles of GSE32453. Subsequently, these differentially expressed genes were subjected to KEGG and GO functional enrichment analysis to explore potential functional mechanisms. The results showed significant enrichment of these differentially expressed genes in aspects such as T cell activation, ion transmembrane transport regulation, extracellular matrix structure, G protein-coupled receptor binding, MAPK signaling pathway, and PI3K-Akt signaling pathway. Additionally, GSEA analysis revealed that HCM genes were mainly enriched in the oxidative phosphorylation signaling pathway and the normalized biological function of respiratory chain complex IV. We also focused on the distribution of immune cells in HCM and found that monocytes, macrophages, and NK cells were the main immune cells infiltrating HCM myocardial tissues. Subsequently, 10 genes closely related to HCM were identified through PPI network analysis: IL2, FOS, CD86, CD68, CCL2, BDNF, RAC2, PLEK, PIK3R1, and LCP2. After validating the differential genes in the GSE36961 dataset, we determined that FOS, CD86, CD68, BDNF, PIK3R1, PLEK, RAC2, and CCL2 were the most important genes (AUC > 0.8).

Studies have shown that patients with HCM exhibit immune system abnormalities, which may lead to inflammation and activation of immune cells, thereby exacerbating myocardial hypertrophy and fibrosis. Van et al proposed that the transition of monocytes/macrophages from M1/M2 subtypes can significantly influence the progression of inflammation from acute myocardial infarction towards resolution, as well as the transition of myocardial tissue from inflammatory damage towards cardiac repair.[12] Recent research has indicated that the proportion of tissue monocyte/macrophage subgroups significantly impacts the occurrence of inflammatory damage and subsequent myocardial repair following myocardial infarction, elucidating potential mechanisms. Manaf et al demonstrated the potential of recombinant human interleukin-2 (rhIL-2) in mitigating myocardial fibrosis, increasing myocardial infarction, and promoting vascular formation in the peri-infarct zone. The angiogenic effects of rhIL-2 are closely associated with NK cell infiltration, overtransfer of activated NK cells enhances cardiac angiogenesis.[13–15]

FOS, one of the key genes downregulated in its expression, is closely associated with the occurrence and development of myocardial hypertrophy. Xavier et al demonstrated that Sirtuin 3 plays a critical role in controlling the FOS/AP-1 pathway, thereby promoting typical complex fibrotic and inflammatory responses in myocardial cells.[16] RAC2 belongs to the Rho family of GTPases, and the Rac2/cofilin pathway plays a crucial role in the induction of muscle fiber morphology and Z-line disarray in RVOT bigeminy VPCs.[17] PLEK is an important intermediate in the secretion and activation of the pro-inflammatory cytokines TNF α and IL-1 β. PI3K-Akt, as an important inflammatory signalling pathway in the development of HCM disease, may influence the onset and progression of the inflammatory response by regulating the activity of PLEK.[18] The initiation of immune responses can be induced by inflammatory processes. In this context, CD68 and CD86 emerge as two key molecules intertwined with the complex immune system.[19] CD68 is a specific marker for macrophages, particularly in cardiac diseases such as myocardial infarction and myocardial fibrosis. It precisely specifies the areas of macrophage aggregation, actively participating in the clearance of necrotic cells and residual tissue debris.[20,21] Conversely, CD86 interacts with CD28 on T cells, stimulating T cell activation and thus triggering immune responses.[22] In cases of inflammatory heart disease, immune system activation may ultimately lead to attacks on myocardial cells, causing damage to the myocardium.[8] Macrophages have various differentiation subtypes, and they have been shown to have complex interactions with myocardial cells in the immune response, tissue repair, and cardiac remodeling in the heart.[23] CCL2, a member of the CC chemokine family, induces CCL2 production mediated by macrophages through Dectin-2 induction, leading to coronary artery inflammation, indicating its crucial role in immune cell migration and inflammatory processes.[15]

Furthermore, we identified two significantly upregulated genes in the HCM group. Brain-derived neurotrophic factor (BDNF) has been shown to activate macrophages and induce pronounced inflammation in the aging heart, suggesting that overexpression of BDNF may trigger cardiovascular diseases, including HCM.[24] PIK3R1 is a regulatory subunit of phosphatidylinositol 3-kinases (PI3Ks), which plays a crucial role in insulin signaling to maintain cardiac metabolic homeostasis.[25] Martin et al investigated the impact of PIK3R1 on the insulin signaling pathway in model mice and found that reducing gene levels led to the development of dilated cardiomyopathy in mice. This disruption in cardiac

metabolism processes can exacerbate myocardial fibrosis, inflammation, and diastolic dysfunction.[26] Notably, PIK3R1 exhibits significant predictive capability in HCM, suggesting that changes in insulin regulation mediated by PIK3R1 may play a crucial role in the progression of HCM.

We validated our sequencing results using immunohistochemical data and single-cell transcriptome data from the HPA database. Based on our findings, it can be inferred that key genes are mainly concentrated in cardiomyocytes, smooth muscle cells, and fibroblasts. Subsequently, we performed qRT-PCR on eight essential genes in the HCM and control groups. Compared to the control group, only the mRNA levels of five genes (CD86, BDNF, PIK3R1, PLEK, RAC2) showed statistically significant differences in the HCM group ($P < 0.05$). The mRNA levels of the other three genes (FOS, CD68, CCL2) differed between the HCM and control groups, but the differences were not statistically significant. The discrepancies between sequencing and qRT-PCR results may stem from inherent cellular heterogeneity during the validation of differential genes and differences between actual samples, leading to nonsignificant trends in certain genes.

However, further experimental validation is needed to determine whether these genes are the primary drivers of HCM. Additionally, our study primarily focused on genes within modules with the highest correlations, overlooking some key genes in other interrelated modules. This constitutes another limitation of our study. Our research is based on bioinformatic immune infiltration analysis of transcriptomic profiles from public datasets, which may not fully reflect the actual scenario. Furthermore, although we analyzed the GSE32453 dataset, the available input data may still be insufficient to accurately screen and identify central genes of HCM. The exact roles of these eight essential genes in the myocardial tissue environment require further investigation, necessitating more molecular research.

Conclusions

HCM shares a close connection with the immune system. Consequently, therapies focusing on the immune system could better HCM, boost heart performance, and slow down the advancement of the disease. The research we conducted did more than just pinpoint eight genes crucial in the emergence and progression of HCM; it also delved deeply into their functional mechanisms, particularly those associated with immune infiltration. The extensive investigation has pinpointed possible biomarkers and routes intimately linked to immune reactions, uncovering the complex and detailed immune terrain underlying HCM.

Data Sharing Statement

The datasets examined in the present study are obtainable. Capable of being stored in the GEO database (http://www.ncbi.nlm.nih.gov/geo/). All data produced throughout this research are provided within this article and its supplementary files. The corresponding author can be contacted for access to the data upon reasonable request.

Ethics Approval and Consent to Participate

GEO and HPA belong to public databases. The patients involved in the database have obtained ethical approval. Users can download relevant data for free for research and publish relevant articles. According to China's "Measures for Ethical Review of Life Science and Medical Research Involving Humans", our study is based on open-source data, so there are no ethical issues.

Acknowledgments

We are deeply grateful to everyone in the laboratory who provided us with assistance.

Author Contributions

All authors made a significant contribution to the work reported, whether that is in the conception, study design, execution, acquisition of data, analysis and interpretation, or in all these areas; took part in drafting, revising or critically reviewing the article; gave final approval of the version to be published; have agreed on the journal to which the article has been submitted; and agree to be accountable for all aspects of the work.

Funding

This study was supported by the Key Research and Development Project of Jiangsu Province (BE2022692 and BE2023652), the Nanjing Important Science & Technology Specific Projects (2021-11005), Nanjing International, Hong Kong, Macao and Taiwan Science and Technology Cooperation Program project (202308001), Nanjing Science and Technology Development Plan Project (202205066), Nanjing Drum Tower Hospital Clinical Research Special Fund project (2023-LCYJ-MS-13) and Nanjing Jiangning District Science and Technology Beneficiary Programme Project (2023027S).

Disclosure

The authors report no conflicts of interest in this work.

References

1. Tuohy CV, Kaul S, Song HK, Nazer B, Heitner SB. Hypertrophic cardiomyopathy: the future of treatment. *European J of Heart Fail*. 2020;22(2):228–240. doi:10.1002/ejhf.1715
2. Owens AT, Cappola TP. Recreational exercise in hypertrophic cardiomyopathy. *JAMA*. 2017;317(13):1319. doi:10.1001/jama.2017.2584
3. Semsarian C, Ingles J, Maron MS, Maron BJ. New perspectives on the prevalence of hypertrophic cardiomyopathy. *J Am College Cardiol*. 2015;65(12):1249–1254. doi:10.1016/j.jacc.2015.01.019
4. Wooten EC, Hebl VB, Wolf MJ, et al. Formin homology 2 domain containing 3 variants associated with hypertrophic cardiomyopathy. *Circ Cardiovasc Genet*. 2013;6(1):10–18. doi:10.1161/CIRCGENETICS.112.965277
5. Lang. Recommendations for cardiac chamber quantification by echocardiography in adults: an update from the American Society of Echocardiography and the European Association of Cardiovascular Imaging. *Eur Heart J Cardiovasc Imaging*. 2016;17(4):412. doi:10.1093/ehjci/jew041
6. Ito T, Suwa M. Echocardiographic tissue imaging evaluation of myocardial characteristics and function in cardiomyopathies. *Heart Fail Rev*. 2021;26(4):813–828. doi:10.1007/s10741-020-09918-y
7. Maron BJ, Rowin EJ, Maron MS. Paradigm of sudden death prevention in hypertrophic cardiomyopathy. *Circ Res*. 2019;125(4):370–378. doi:10.1161/CIRCRESAHA.119.315159
8. Saparov A, Ogay V, Nurgozhin T, et al. Role of the immune system in cardiac tissue damage and repair following myocardial infarction. *Inflamm Res*. 2017;66(9):739–751. doi:10.1007/s00011-017-1060-4
9. Maron BJ, Gardin JM, Flack JM, Gidding SS, Kurosaki TT, Bild DE. Prevalence of hypertrophic cardiomyopathy in a general population of young adults: echocardiographic analysis of 4111 subjects in the CARDIA study. *Circulation*. 1995;92(4):785–789. doi:10.1161/01.CIR.92.4.785
10. Chen CY, Lin LY, Lin YH, et al. P5269The impact of sarcomeric mutations on myocardial fibrosis and ventricular diastolic function in hypertrophic cardiomyopathy (SADS-TW HCM registry study). *Euro Heart J*. 2019;40(Supplement_1):ehz746. doi:10.1093/eurheartj/ehz746.0240
11. Fumagalli C, Fedele E, Beltrami M, et al. P1243Comparison of long-term clinical course and outcome of MYBPC3 - versus MYH7 - related hypertrophic cardiomyopathy. *Euro Heart J*. 2019;40(Supplement_1):ehz748. doi:10.1093/eurheartj/ehz748.0201
12. Van Den Akker F, Deddens JC, Doevendans PA, Sluijter JPG. Cardiac stem cell therapy to modulate inflammation upon myocardial infarction. *Biochimica et Biophysica Acta*. 2013;1830(2):2449–2458. doi:10.1016/j.bbagen.2012.08.026
13. Imanaka-Yoshida K. Inflammation in myocardial disease: from myocarditis to dilated cardiomyopathy. *Pathol Int*. 2020;70(1):1–11. doi:10.1111/pin.12868
14. Frantz S, Hofmann U, Fraccarollo D, et al. Monocytes/macrophages prevent healing defects and left ventricular thrombus formation after myocardial infarction. *FASEB J*. 2013;27(3):871–881. doi:10.1096/fj.12-214049
15. Bouchentouf M, Williams P, Forner KA, et al. Interleukin-2 enhances angiogenesis and preserves cardiac function following myocardial infarction. *Blood*. 2010;116(21):2786. doi:10.1182/blood.V116.21.2786.2786
16. Palomer X, Román-Azcona MS, Pizarro-Delgado J, et al. SIRT3-mediated inhibition of FOS through histone H3 deacetylation prevents cardiac fibrosis and inflammation. *Sig Transduct Target Ther*. 2020;5(1):14. doi:10.1038/s41392-020-0114-1
17. Lin YS, Chang TH, Ho WC, et al. Sarcomeres morphology and Z-line arrangement disarray induced by ventricular premature contractions through the Rac2/cofilin pathway. *IJMS*. 2021;22(20):11244. doi:10.3390/ijms222011244
18. Shimada YJ, Raita Y, Liang LW, et al. Comprehensive proteomics profiling reveals molecular pathways that are differentially regulated in hypertrophic cardiomyopathy and correlate with clinical markers of disease severity. *Euro Heart J*. 2021;42(Supplement_1):ehab724. doi:10.1093/eurheartj/ehab724.1777
19. Talaat IM, Elemam NM, Abdullah HW. CD68, CD86 and CD163 expression profile in breast cancer molecular subtypes. *THE FASEB J*. 2022;36(S1):1. doi:10.1096/fasebj.2022.36.S1.R3106
20. Ryabov V, Gombozhapova A, Rogovskaya Y, Kzhyshkowska J, Rebenkova M, Karpov R. Cardiac CD68+ and stabilin-1+ macrophages in wound healing following myocardial infarction: from experiment to clinic. *Immunobiology*. 2018;223(4–5):413–421. doi:10.1016/j.imbio.2017.11.006
21. Loi H, Kramar S, Laborde C, et al. Metformin attenuates postinfarction myocardial fibrosis and inflammation in mice. *IJMS*. 2021;22(17):9393. doi:10.3390/ijms22179393
22. Motta M, Shelvin B, Lerner S, Keating M, Wierda WG. Increased Expression of CD152 by normal T lymphocytes in untreated patients with B cell chronic lymphocytic leukemia. *Blood*. 2004;104(11):963. doi:10.1182/blood.V104.11.963.963
23. Psarras S, Beis D, Nikouli S, Tsikitis M, Capetanaki Y. Three in a box: understanding cardiomyocyte, fibroblast, and innate immune cell interactions to orchestrate cardiac repair processes. *Front Cardiovasc Med*. 2019;6:32. doi:10.3389/fcvm.2019.00032
24. Cai D, Holm JM, Duignan IJ, et al. BDNF-mediated enhancement of inflammation and injury in the aging heart. *Physiological Genomics*. 2006;24(3):191–197. doi:10.1152/physiolgenomics.00165.2005

25. Zhang L, Jain MK. Circadian regulation of cardiac metabolism. *J Clin Invest*. 2021;131(15):e148276. doi:10.1172/JCI148276
26. Young ME, Brewer RA, Peliciari-Garcia RA, et al. Cardiomyocyte-specific BMAL1 plays critical roles in metabolism, signaling, and maintenance of contractile function of the heart. *J Biol Rhythms*. 2014;29(4):257–276. doi:10.1177/0748730414543141